http://communications.science.ankara.edu.tr

Commun.Fac.Sci.Univ.Ank.Series A2-A3
Volume 64, Number 1, Pages 21-39 (2022)
DOI: 10.33769/aupse.1068297
ISSN 1303-6009 E-ISSN 2618-6462

Research Article; Received: Feburary 04, 2022; Accepted: Feburary 24, 2022

THE EFFECTS OF DC OFFSET IN DIRECT-CONVERSION RECEIVERS FOR WLAN SYSTEMS

Yunus Emre ŞEN[1] and Selçuk TAŞCIOĞLU[2]

[1]Department of Electrical and Electronics Engineering,
Gazi University, Ankara, TURKEY
[2]Department of Electrical and Electronics Engineering,
Ankara University, Ankara, TURKEY

ABSTRACT. In this paper, the effects DC offset in direct-conversion receivers for WLAN systems are analyzed using both experimental and simulation data. DC offset estimation is performed by using data-aided methods which are based on the short training sequence of WLAN preamble. In the simulations, DC offset and frequency offset estimations are carried out on the signals affected by frequency selective Rayleigh fading channel and additive white Gaussian noise. Estimation performance of the methods is compared for different SNR levels and frequency offset values in terms of mean square error. Experimental data which is in the form of WLAN packets and transmitted through a wireless channel is captured by using a software defined radio. The experimental performance of the DC offset compensation methods is evaluated in terms of transmission success ratio.

1. INTRODUCTION

With the increasing demand for mobile communication and the reduction in the size of wireless communication devices over time have led to some developments in receiver architectures. As a result of these developments, new generation receivers with simpler architecture and lower power consumption have emerged. The most popular receiver architecture with these features is the direct-conversion receiver architecture [1]. Unlike traditional heterodyne receivers, nonintegrable RF filters are not required in direct-conversion receivers, which reduces the cost and dimension of the system. However, these receivers have some disadvantages caused by their architecture which reduces the system performance. The advantages and disadvantages of traditional and new generation wireless receiver architectures have

Keywords. DC offset, direct-conversion receivers, frequency offset, WLAN, software defined radio.
yunusemresen@gazi.edu.tr; selcuk.tascioglu@eng.ankara.edu.tr-Corresponding author
0000-0001-5103-3388; 0000-0001-9064-2960.

been discussed considering compatibility with the integrated circuits in [1,2]. Designing issues of the direct-conversion receivers were described and circuit techniques for alleviating the disadvantages of this architecture were proposed in [3].

One of the most serious problems of direct-conversion receivers is the DC offset which causes distortion when the RF spectrum is downconverted to the baseband [4]. Large values of the DC offset would saturate the receiver front-end, which may cause the signal not to be properly amplified. Therefore, the DC offset significantly affects the dynamic range of the receiver and accordingly its sensitivity. Even a small amount of DC offset, if not compensated, may degrade the performance of a direct-conversion receiver by causing estimation errors for the parameters in detection and decoding stages [5]. Besides, the performance loss due to DC offset is expected to be more serious for high order modulation techniques [5]. Therefore, DC offset should be properly compensated in direct-conversion receivers working in wireless networks to provide a reliable communication, especially at high data rates where high order modulation is required.

DC offset arises in direct-conversion receivers due to different reasons. Basically, the leakage signals that occur as a result of the imperfect isolation between the components in the receiver circuit generate DC offset [2,3]. Due to imperfect isolation in the receiver, the local oscillator (LO) signal leaks from the mixer and appears at the input of the mixer on the low noise amplifier (LNA) side as shown in Fig. 1. The leakage signal is multiplied by itself, which is called self-mixing. Depending on impedances between the components in the receiver, the leakage signals may be observed at the input of the mixer, as well as they may be transmitted from the antenna and reflected from the objects in the environment and returned to the receiver again. DC offset is also observed when a large interference signal leaks into the local oscillator port and is multiplied by itself at the mixer [3]. Leakage signals causing DC offset are shown in Fig. 1. In this figure, dashed curves denote leakage signals and dotted curve indicates interference signal.

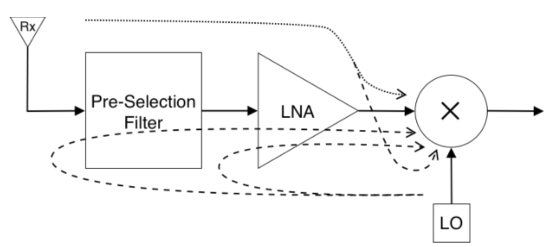

FIGURE 1. Origin of DC offset [2].

In order to increase the performance of the direct-conversion receivers, DC offset may be compensated by using analog or digital signal processing methods. In analog methods, an ideal DC offset cancellation circuit is desired to act as a high-pass filter with an infinite attenuation at the DC, while passing the desired signal spectrum without distortion [6]. These methods simultaneously update the estimates as the DC offset changes in time, which makes them attractive for real time applications. The simplest analog method is AC-coupling which uses a DC block capacitor and a resistor to form a high-pass filter character. This method can be used for modulation schemes where the spectrum of the signal is located away from DC. However, circuit design with the requirement of low attenuation on the desired band increase the power consumption and chip area, which is not suitable for new generation low-cost receivers [6].

In order to simplify the circuit design and increase the integration level of the receivers, several digital signal processing techniques have been employed [5, 7-11]. In these methods, DC offset estimation task has been performed after digitizing the signal by an analog-to-digital converter.

In [7], a digital signal processing technique based on least-squares estimation was proposed to mitigate the effects of DC offset and IQ mismatch in direct-conversion receivers. It was shown by simulations that the method has a good performance for frequency-selective channels. In [8], IQ imbalance, DC offset, and channel response were estimated jointly for an orthogonal frequency division multiplexing (OFDM) system. The estimations were performed by one OFDM block which is arbitrarily chosen for training. The authors demonstrated through simulations that the performance of the proposed method was similar to the performance in case of perfect information about these parameters. In [9-11], data-aided DC offset estimation methods which can be employed in OFDM based WLAN systems were proposed.

In this paper, three existing DC offset estimation methods for OFDM-based WLAN systems have been implemented and compared through simulations in terms of mean square error (MSE). We also implemented the mean subtraction approach on WLAN signals for a baseline comparison. The effect of DC offset cancellation methods on the wireless communication performance in a real system has also been measured. The experimental performance evaluation of the methods has been obtained by applying the methods to the signals transmitted by a software defined radio.

The outline of the paper is as follows: In Section 2, problem definition for DC offset problem is introduced. In Section 3, carrier frequency offset estimation methods used in this paper are presented. In Section 4, motivation for why CFO and DC offset problems should be addressed together is explained and DC offset estimation methods used in this paper are given. Simulation and experimental results are presented in Section 5 and Section 6, respectively. Section 7 concludes the paper.

2. Problem Definition

The discrete baseband signal model for one OFDM symbol length excluding the cyclic prefix is given by

$$y(n) = h(n) * x(n) + w(n) + d, \quad n = 1,2,\ldots,N \tag{1}$$

where n is discrete time index, N is the number of subcarriers in the OFDM system, $x(n)$ denotes transmitted signal, $h(n)$ and $w(n)$ are additive white Gaussian noise and channel response, respectively, and d is the DC offset. For the direct conversion receiver architecture, quadrature mixing is used in which real DC offset occurs in quadrature branches. Quadrature signals are represented as $I + jQ$ to form the complex baseband signal for digital signal processing, in which case DC offset is also represented as a complex number. Mathematical expression for the DC offset resulting from the self-mixing can be given as

$$A_1\cos(\omega_{LO}t)A_2\cos(\omega_{LO}t) = \underbrace{\frac{A_1A_2}{2}}_{DC\ Term} + \frac{A_1A_2}{2}\cos(2\omega_{LO}t) \tag{2}$$

where sinusoidal terms at the left hand side of the equation are LO signal and leakage version of this signal at the input of the mixer. A_1 and A_2 are the amplitudes and ω_{LO} is the frequency of these signals. This multiplication results in a high frequency and a DC term. The high frequency term can be removed by filtering out since the desired signal is downconverted to the baseband, however the DC component causes a distortion when the desired signal contains energy at DC.

In this paper, DC offset problem and the compensation methods are considered for the OFDM based WLAN signals having non-high throughput (non-HT) transmission vector format preambles [12]. The data-aided compensation methods considered herein use a part of the legacy short training field (L-STF) of the WLAN preamble. This signal part is extracted from the first OFDM symbol by removing the cyclic prefix. For channel bandwidth of 20 MHz and $N = 64$ subcarriers, L-STF is constructed from two identical OFDM symbols of length 160 samples. After removing the 16-length cyclic prefix from the first OFDM symbol, the signal part used for DC offset estimation is obtained as

$$r = \left[y(17) \ \ldots \ y(80) \right]^T \tag{3}$$

Time domain average of the received signal is defined as follows

$$\widehat{d} = \sum_{n} y(n) \tag{4}$$

(4) can be used as a DC offset estimation and DC component can be simply eliminated using mean subtraction (MS) approach. This approach is used in the literature in various forms. For example, in [13] DC offset is estimated by using a blind method having two stages. At the first stage of this method, mean subtraction is carried out and it has been emphasized that it provides a coarse compensation. The formulation for the compensated signal $\boldsymbol{r}_0$ is given as

$$\boldsymbol{r}_0 = \left\{ \boldsymbol{I}_{N\times N} - (1/N)\, \boldsymbol{a}\boldsymbol{a}^H \right\} \boldsymbol{r} \tag{5}$$

where N=64 is the length of signal $\boldsymbol{r}$, $\boldsymbol{\alpha}$ is 64-length column vector whose all elements are equal to 1, $\boldsymbol{I}$ is 64×64 identity matrix, and $(\,.\,)^H$ denotes the Hermitian transpose of a matrix.

In this paper, mean subtraction approach is applied to 64-length L-STF signal as in other implemented methods. In this case, DC offset estimation by mean subtraction is calculated as

$$\widehat{d} = \sum_{n=0}^{N-1} r(n) \tag{6}$$

where $r(n)$ is 64-length L-STF signal part which is defined in (3).

Even though mean subtraction is easy to implement, DC offset estimation performance of this method is not good enough. Therefore, it would not be the best choice for WLAN systems. The aim of implementing the mean subtraction method is to compare the performances of the DC offset compensation methods with the performance of this baseline approach. Also, this method cannot be implemented when using a modulation scheme having DC. DC subcarrier is not used in OFDM based WLAN protocols discussed in this paper. However, for these systems there is another issue called carrier frequency offset (CFO), which must be compensated to avoid reducing system performance. Without cancelling the DC offset with a high accuracy, CFO compensation causes spreading the DC energy over the other subcarriers [5]. Therefore, CFO and DC offset problems should be addressed together. The CFO compensation can be performed after cancelling the DC offset from the received signal as follows

$$\widehat{y}(n) = (y(n) - \widehat{d})\, e^{-j2\pi n\widehat{\varepsilon}/N}, \quad n = 1, 2, \ldots, N \tag{7}$$

In the following sections CFO and DC offset estimation methods used in this paper are presented.

3. Carrier Frequency Offset Estimation

OFDM provides high data rates by using overlapping subcarriers, which makes it a common technique for WLAN systems. However, the use of overlapping subcarriers increases vulnerability to the CFO caused by the Doppler shift and the frequency mismatch between the local oscillator signals at the receiver and transmitter. The existence of CFO leads to intercarrier interference (ICI) whose effect is shown in Fig. 2 for L-STF spectrum. This figure shows that the amount of distortion changes with CFO value.

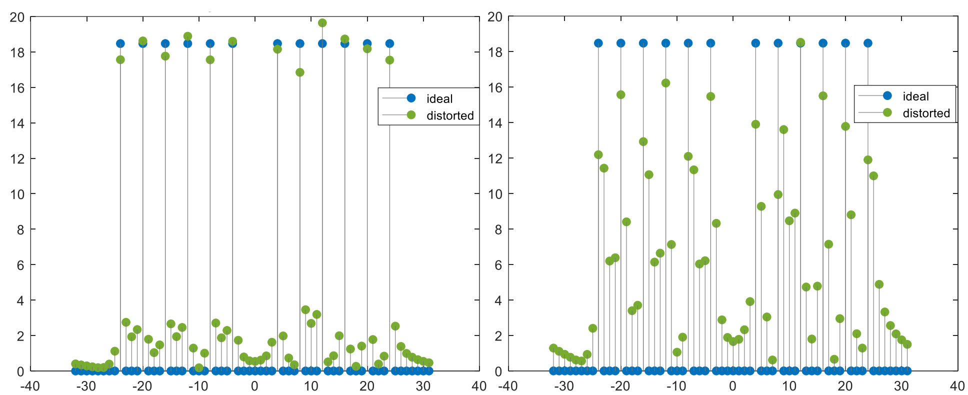

FIGURE 2. Distortions caused by CFO on L-STF spectrum for CFO vales of 0.1 (left) and 0.4 (right).

In this paper, simulations and experiments were performed for WLAN system with 20 MHz channel bandwidth. In this case, spacing between OFDM subcarriers is found to be as 20 MHz / 64 = 312500 Hz. Using this value, the normalized CFO is calculated as

$$\varepsilon = \frac{\Delta f}{312500} \tag{8}$$

where Δf is the CFO value in Hz.

Two different CFO estimation methods have been implemented in this paper. The first method proposed in [9] employs the same part of L-STF signal which is used for DC offset estimation and defined in (3). Two signal parts are taken from $\boldsymbol{r}$

defined as $\boldsymbol{r}_1 = [r(0), \ldots, r(48)]$ and $\boldsymbol{r}_2 = [r(16), \ldots, r(64)]$. A complex scalar R_p value is calculated from these signal parts as follows

$$R_p = L^{-1} \boldsymbol{r}_1^H \boldsymbol{r}_2 - L^{-2} \boldsymbol{r}_1^H \mathbf{1}_L \mathbf{1}_L^T \boldsymbol{r}_2 \tag{9}$$

where L is the length of $\boldsymbol{r}_1$ ve $\boldsymbol{r}_2$ vectors, $\mathbf{1}_L$ is an all 1 vector, and $(\ .)^T$ denotes the transpose of a matrix. By using the complex R_p value, CFO is estimated by

$$\hat{\varepsilon} = \frac{M}{2\pi} arg\left(R_p\right) \tag{10}$$

where M denotes the number of identical symbols in an OFDM symbol excluding the cyclic prefix and $arg(\ .)$ represents the argument of a complex number. CFO estimation can be performed in the matrix form as follows

$$\boldsymbol{r}_0 = \boldsymbol{\Gamma}_N(\hat{\varepsilon})\ \boldsymbol{r} \tag{11}$$

where $\boldsymbol{\Gamma}_N$ represents diagonal matrix defined as

$$\boldsymbol{\Gamma}_N(\hat{\varepsilon}) = diag\left\{1, e^{j\frac{2\pi\hat{\varepsilon}}{N}}, \ldots, e^{j\frac{2\pi\hat{\varepsilon}(N-1)}{N}}\right\} \tag{12}$$

CFO estimation was also carried out by using a second method which is given in the Matlab WLAN toolbox [14]. There are two CFO estimation stages namely coarse and fine in this approach. The L-STF and L-LTF fields of the WLAN preamble are used for coarse and fine CFO estimations, respectively. The sum of these estimations is subtracted from the entire WLAN packet to perform CFO compensation.

4. DC Offset Estimation

The DC subcarrier is not used in OFDM based WLAN protocols in order to mitigate the distorting effect caused by DC offset [12]. DC offset would be easily cancelled by the mean subtraction approach if there were no CFO. However, in the presence of CFO, some part of the energy of other subcarriers carrying information leaks into the DC subcarrier. If the mean value of the signal is subtracted from itself, the information shifted to the DC region will be lost. That would reduce the system performance. Therefore, more effective DC offset estimation methods should be employed.

Fig. 3 shows the effects of distortions resulting from DC offset and CFO on L-STF spectrum as well as resulting spectrums after compensation for the CFO value of 0.4. For this visualization, DC offset is taken as 0.3+*j*0.3 so that DC offset is stronger than the other subcarriers. In this way, it is aimed to observe the distorting effect clearly when the DC spreads over the other subcarriers due to CFO compensation. In this figure, blue points represent ideal spectrum when there are no distorting effects and green points denote the distorted spectrums. The signals distorted by CFO resulting from moving objects in the wireless environment, DC offset is superimposed on this signal at the direct-conversion receiver. Note that the distorted spectrums in Fig 3 (green points) are the sum of the DC offset and the distorted spectrums due to CFO in Fig. 2.

Fig. 3 also shows the compensated spectrums (red points). In the top left figure, the effect of compensation of CFO without DC offset cancellation is shown. As can be seen from this figure, CFO compensation spreads the DC energy over the other subcarriers. This will degrade the system performance. In the top right figure, the case where DC offset is estimated with a high estimation error and is cancelled prior to CFO compensation is considered. In this case the effect of DC energy over the other subcarriers is reduced compared to the case in the figure on the top left as expected. Since the estimated DC offset is removed from the signal prior to CFO compensation. For the bottom left figure, DC offset estimation is performed by using mean subtraction method. This method removes all the energy at DC including the useful energy which leaks from other subcarriers. Note that the DC component contains not only the DC offset but also the useful energy leaks from other subcarriers due to CFO. Removing this useful information causes distortion after DC offset and CFO compensations, especially at the subcarriers around DC. These distortions can be seen in the figure on the bottom left by comparing the compensated red points with the ideal blue points. Note that the subcarriers around DC are null for L-STF signal, but are used in data symbols. Therefore, this distortion may result in an increased bit error rate. Lastly, in the bottom right figure, the case where DC offset is estimated perfectly is considered. As shown from this figure, after compensating the DC offset and CFO perfectly, ideal spectrum is recovered without any loss. These figures show that the accuracy of DC offset estimation has a significant impact on the information carrying subcarriers and thus overall system performance for an OFDM based WLAN system.

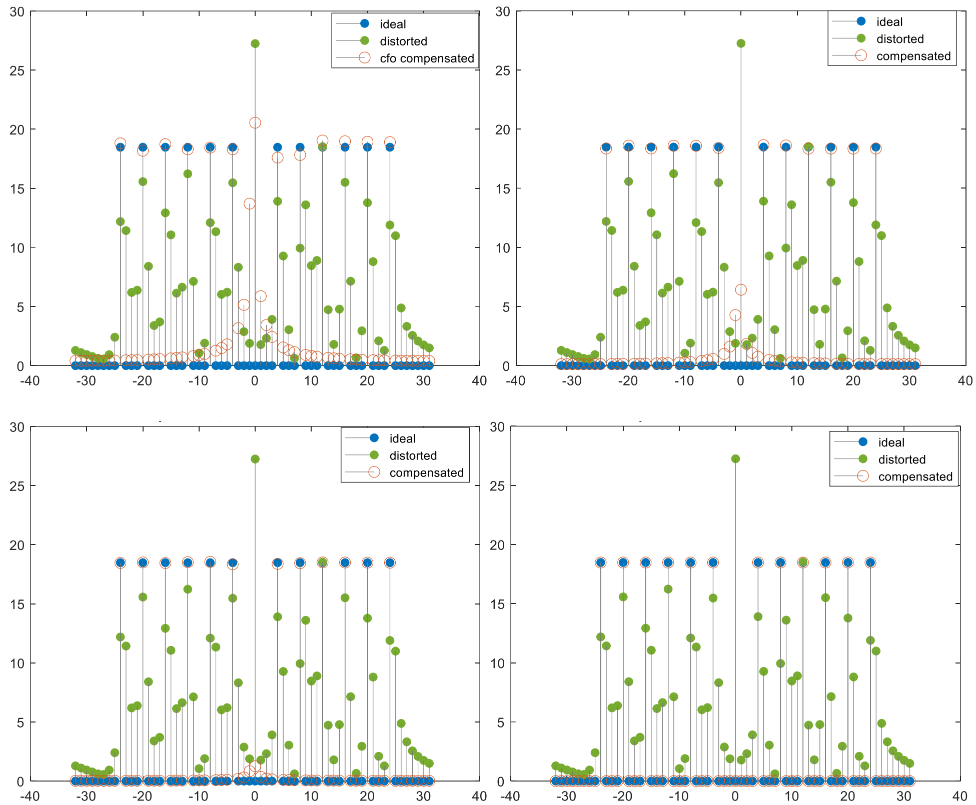

FIGURE 3. L-STF spectrums for ideal (blue), distorted (green) and compensated (red) cases. Top left: CFO compensation is performed without DC offset (DCO) cancellation. Top right: DC offset is estimated with a high estimation error and then CFO is compensated. Bottom left: DC offset estimation is performed by using mean subtraction method (MS) prior to CFO compensation. Bottom right: DC offset is estimated perfectly prior to CFO compensation.

Spectrums of two WLAN signals with (top) and without (bottom) DC offset compensation are given in Fig. 4. In the case where the DC offset is not compensated, an increase of approximately 50 dBm is observed in the power of the DC component compared to the compensated case.

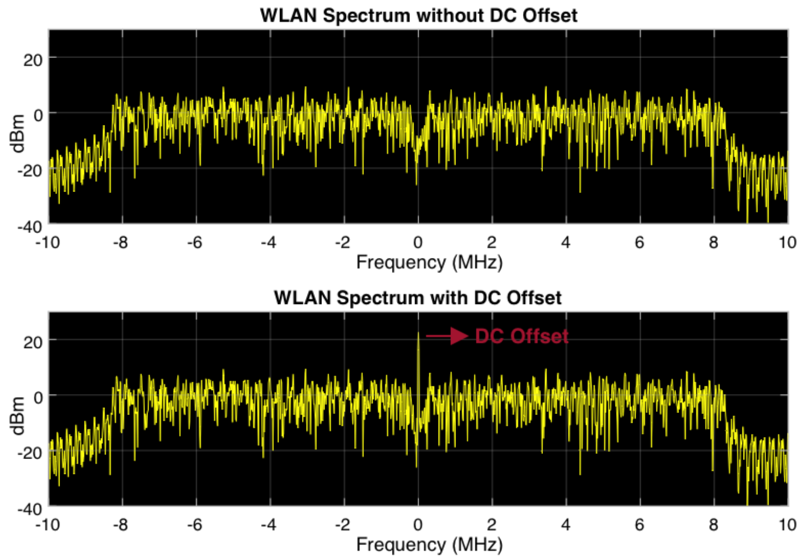

FIGURE 4. WLAN spectrum for the cases with (top) and without (bottom) DC offset compensation.

4.1. **Joint Estimation of DC Offset and CFO.** In order to achieve high performance in WLAN systems, CFO and DC offset compensations should be considered together. A method using this approach is suggested by Lin *et al*. in [9]. In this method, the estimation of the DC offset is performed by using the estimation value of CFO. Thus, high DC offset estimation performance can be achieved independent of CFO values. After estimating offset values, DC offset and CFO compensations are carried out respectively. All unloaded subcarriers are used in this method for DC offset estimation. Therefore, even at low CFO values, the energy contained in the loaded subcarriers may leak to the unloaded subcarriers used for DC offset estimation. For this reason, the CFO estimation is taken into account in the estimation of the DC offset in order to improve the estimation accuracy of the DC offset.

In this method, DC offset is estimated as

$$\hat{d} = \left[\boldsymbol{V}^H \boldsymbol{\Gamma}_N^H(\hat{\varepsilon})\, \mathbf{1}_N\right]^{\dagger} \boldsymbol{V}^H \boldsymbol{\Gamma}_N^H(\hat{\varepsilon})\, \boldsymbol{r} \tag{13}$$

where $\boldsymbol{r}$ is 64-point L-STF signal, $\boldsymbol{\Gamma}_N^H$ is the Hermitian transpose of the diagonal matrix defined in (12), $\dagger$ denotes the pseudo inverse of the matrix, $\mathbf{1}_N$ is an all 1 vector, $\hat{\varepsilon}$ is the estimated normalized CFO. $\boldsymbol{V}$ is the partition of the inverse DFT matrix $\boldsymbol{W}$ containing only the columns corresponding to unloaded subcarriers, which can be defined as

$$\boldsymbol{V}=\left[W_{N_{1:4}}\ W_{N_{6:8}}\ \dots\ W_{N_{26:40}}\ \dots\ W_{N_{58:60}}\ W_{N_{62:64}}\right] \tag{14}$$

where $W_{N_{s:t}}$ represents the columns of inverse DFT matrix corresponding to unloaded subcarriers between indices s and t. Inverse DFT matrix is defined as

$$W_N=\frac{1}{\sqrt{N}}\begin{bmatrix} 1 & 1 & \cdots & 1 \\ 1 & e^{j\frac{2\pi}{N}} & \cdots & e^{j\frac{2\pi(N-1)}{N}} \\ \vdots & \vdots & \ddots & \vdots \\ 1 & e^{j\frac{2\pi(N-1)}{N}} & \cdots & e^{j\frac{2\pi(N-1)(N-1)}{N}} \end{bmatrix} \tag{15}$$

4.2. **DC Offset Estimation via Mitigating the Effect of ICI on DC Subcarrier.** The existence of CFO results in intercarrier interference (ICI) as explained in Section 3. In the L-STF field of the WLAN preamble, DC subcarriers and adjacent 3 subcarriers on the left and the right are unloaded [12]. Therefore, the amount of energy leaked on subcarriers -1, 0, 1 due to the frequency offset is relatively low and close to each other. If one can estimate the energy level leaked to DC due to ICI, then DC offset estimation can be performed with a high accuracy and independent of CFO. Xia and Ren has implemented this methodology by averaging the values of the subcarriers -1 and 1, then subtracting it from the DC component as follows [10]

$$\widehat{d}=\left[Y_0-\left(Y_1+Y_{-1}\right)/2\right]/\sqrt{N} \tag{16}$$

The values of the subcarriers -1, 0, and 1 are calculated by using the DFT formula given as

$$Y(k)=\frac{1}{\sqrt{N}}\sum_{n=0}^{N-1} r_n e^{-j2\pi nk/N}, \quad k=-1,0,1 \tag{17}$$

The robustness of this method is based on the fact that the amount of the leakage energy on the DC subcarrier due to ICI can be estimated with a high accuracy by averaging the values of subcarriers -1 and 1. Note that the amount of the leakage energy on the subcarriers -1, 0, and 1 are low and close to each other since the loaded

L-STF subcarriers are sparsely located. This approach provides a DC offset estimation independent of the amount of CFO.

4.3. **DC Offset Estimation Using Linear Unbiased Estimator.** In [11], Marsili has proposed a linear unbiased estimator for DC offset estimation. This method uses the estimation coefficients defined as

$$\boldsymbol{a} = \frac{1}{\mathbf{1}^T \boldsymbol{C}^{-1} \mathbf{1}} \{ \boldsymbol{C}^{-1} \mathbf{1} \} \tag{18}$$

where $\boldsymbol{C}$ is the correlation matrix, $(\,.\,)^{-1}$ denotes the inverse of a matrix, $\mathbf{1}$ is the $N \times 1$ vector whose elements are equal to 1. The correlation matrix contains the information about the WLAN preamble and CFO information which is modeled as a uniform random variable. By using the estimation coefficients defined in (18), DC offset is estimated as

$$\widehat{d} = \boldsymbol{a}^T \boldsymbol{r} \tag{19}$$

Since the CFO is modeled as a random variable in this method, the performance of the method is based on the interval defined for this random variable. That means the performance of the method increases as the prior information about CFO increases.

5. Simulation Results

In simulations, 64 QAM OFDM based WLAN signals with non-HT preambles were generated and passed through a frequency selective Rayleigh fading channel with 6 paths. The channel has an exponential power delay profile, a root mean square (RMS) delay spread of 100 ns [10] and 50 Hz maximum Doppler shift. Additive white Gaussian noise was added to the generated signals to simulate different SNR levels after adding CFO and DC offset. CFO and DC offset estimations were performed and estimation performances were evaluated using mean square error (MSE). MSE values were calculated over 10000 Monte Carlo iterations in each of which noise and channel were generated randomly.

5.1. **CFO Estimation Performance.** The performances of CFO estimation methods were compared for different SNR and CFO values in terms of MSE. As seen from Fig. 5, the performance of the Lin's method in [9] remains the same with varying CFO values. The MSE performance of the estimator in Matlab WLAN toolbox, which has two stages as explained in Section 3, increases for integer-valued CFOs and is the similar to the Lin's method for the CFO values away from integers. The performance of both the methods significantly decreases at the normalized CFO values of -2 and 2. This can be explained as the energy of the subcarriers carrying information in the L-STF spectrum shown in Fig. 2 is shifted to the center point of these subcarriers as a result of CFO. In this case the estimation errors take the largest values.

The effect of SNR on the MSE performance of the CFO estimation methods was also evaluated for two different CFO values of 0.4 and 0.001. The performance of the Lin's method remains the same as the CFO values change in the interval [-1.9, 1.9]. The performance of the method defined in Matlab WLAN toolbox increases as the SNR increases for the normalized CFO value of 0.001. When the normalized CFO value is 0.4, the performance remains constant above 20 dB.

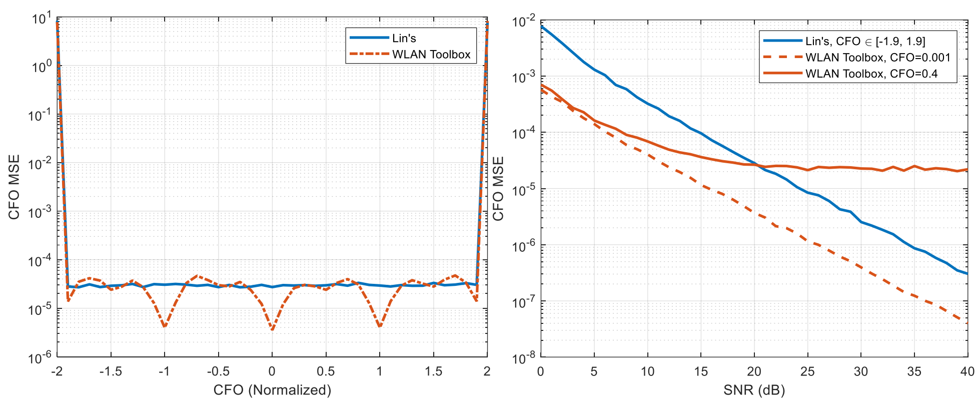

FIGURE 5. MSE of CFO estimation versus CFO (left) and SNR (right) values. DC offset is taken 0.1+*j*0.1 for both cases and SNR is taken as 20 dB for MSE versus CFO graph (left).

5.2. **DC Offset Estimation Performance.** DC offset estimation performances of the methods were evaluated for different CFO values and visualized in Fig. 6 (left). The performances of mean subtraction (MS) approach and Marsili's method [11] depend on the CFO values, whereas Lin's [9] and Xia's [10] methods are independent of CFO values. This can be explained by the fact that CFO is not estimated in the subtract mean approach and Marsili's method. On the other hand, in Lin's method CFO estimation is used for DC offset estimation. In the Xia's method, the distortion caused CFO is mitigated by using the information provided by three subcarriers -1, 0, and 1. The amount of energy leaking to DC is estimated by averaging the subcarriers -1 and 1, then subtracting them from the DC component. Therefore, the method's performance is independent of CFO. The same figure shows that the performances of the mean subtraction approach and Marsili's method degrade for the CFO values around the center of two subcarriers's frequencies. At these CFO values, the amount of energy leaking to DC due to CFO increases as can be seen from Fig. 2.

The performance of the Marsili's method depends on the prior information about the normalized CFO parameter which is modeled as a uniform random variable in this method. In Fig. 6 (left), taking a large interval for the uniform random variable degrades the performance of the Marsili's method. When there is a strong information about CFO, the interval for the uniform random variable can be decreased which increases the performance of this method.

In Fig. 6 (right) DC offset estimation performance is investigated versus varying DC offset values. MSE remains constant for all the methods as DC offset changes.

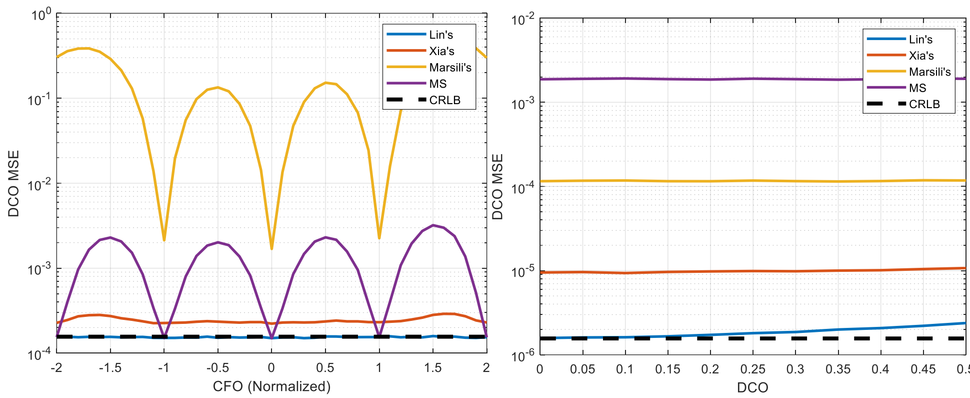

FIGURE 6. MSE of DC offset estimation versus CFO for DCO=0.1+j0.1 and SNR=20 dB (left). MSE of DC offset estimation versus DC offset for CFO=0.4 and SNR=40 dB (right).

DC offset estimation performance was evaluated for varying SNR levels. In these simulations, the CFO values were chosen to be 0.001 and 0.4 in order to observe the effect of CFO values on the DC offset estimation. DC offset is taken as 0.1+j0.1, since the value of DC offset does not change the MSE performance as seen from Fig. 6 (right). MSE of DC offset estimation for two different normalized CFO values are given in Fig. 7. Lin's method has the best estimation performance which is very close to Cramer-Rao Lower Bound (CRLB) [15] as can be seen from Fig. 6 and Fig 7. Xia's method has also a good performance for the considered SNR levels. The underlying reason for this result is that these two methods use more than one unloaded subcarriers which is a strong prior information to estimate DC offset. For the mean subtraction approach, MSE values does not decrease as the SNR level is increased above 20 dB. In this method, only DC subcarrier is used for estimation without considering CFO. In Marsili's method, the interval for normalized CFO parameter was taken as [-1, 1]. This uncertainty limits its performance for high SNR levels.

For the low value of CFO (0.001), the amount of energy leaking to DC is substantially decreased. Therefore, performances of all the methods are increased and very close to the CRLB as seen from Fig. 7 (right). This result is consistent with the result in Fig. 6 (left). For Marsili's method, the interval for the uniform random variable was taken as [-0.1, 0.1]. Note that better performance can be obtained with this method when more specific prior information is provided.

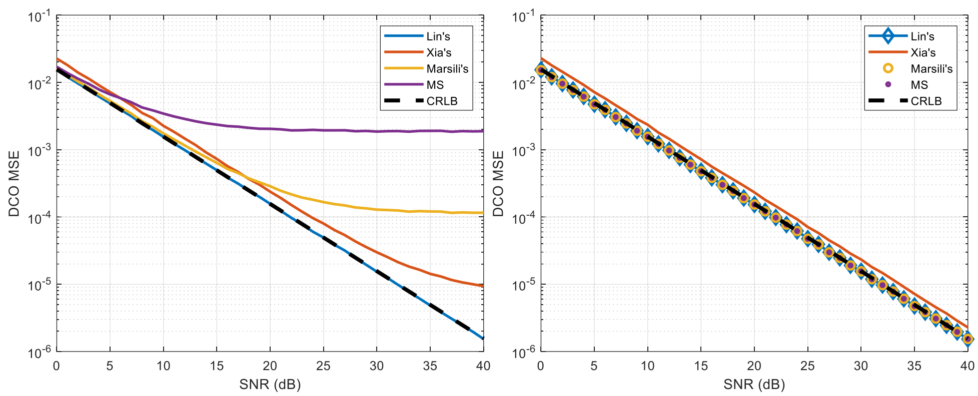

FIGURE 7. MSE of DC offset estimation versus SNR for the CFO values of 0.4 (left) and 0.001 (right) when DC offset is 0.1+j0.1.

6. Experimental Results

The effect of DC offset compensation on the transmission performance in an indoor wireless channel was evaluated through experiments by using a software defined radio (SDR) including receiver and transmitter units, which is shown in Fig 8. A low resolution image was transmitted in the form of IEEE 802.11 packets through the channel and captured by the receiver antenna. Captured RF signals were downconverted to the baseband and digitized by the software defined radio. The decoding process was carried out by using the Matlab WLAN software toolbox [16]. Transmission success rate was calculated by the ratio of number of received images to the number of all transmitted images. Transmissions over the wireless channel were repeated 1000 times and transmission success rates were calculated.

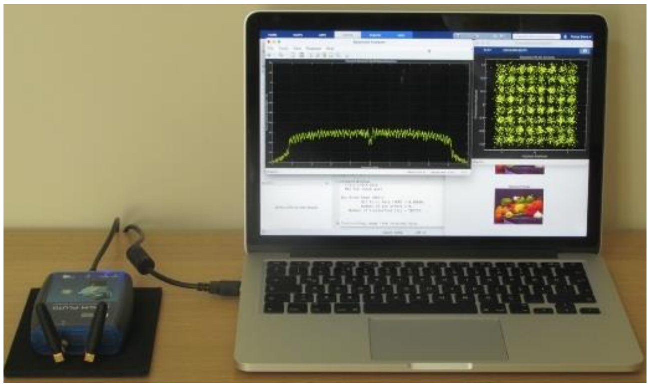

FIGURE 8. Experimental setup consisting of computer and SDR connected via USB 2.0 interface.

In the experiments, DC compensation property of the SDR was turned-off in order to implement the digital signal processing techniques considered in this paper. These methods were applied to the received signals to estimate the DC offset in WLAN packets. The transmission success rate obtained for each method is shown in Fig. 9. From this figure, it can be seen that the transmission success rate is low (23%) in the absence of DC offset compensation. Substantial performance increase was observed when the DC offset was compensated. As seen from the figure, the transmission success rate is over 70% for all the methods.

Digital signal processing methods analyzed herein except the mean subtraction (MS) approach use prior information about the non-HT transmission format such as loaded and unloaded subcarrier indices. Therefore, a better performance is expected with these methods. In this experiment, a result consistent with this expectation was obtained. The experimental performance of the methods for this experiment is similar to the performance obtained by simulations for a low CFO value in Fig 7 (right), since CFO values are low for this experimental setup. However, it should be noted that the observed performance of the methods may vary for different experimental scenarios due to the factors such as interference and multipath effects.

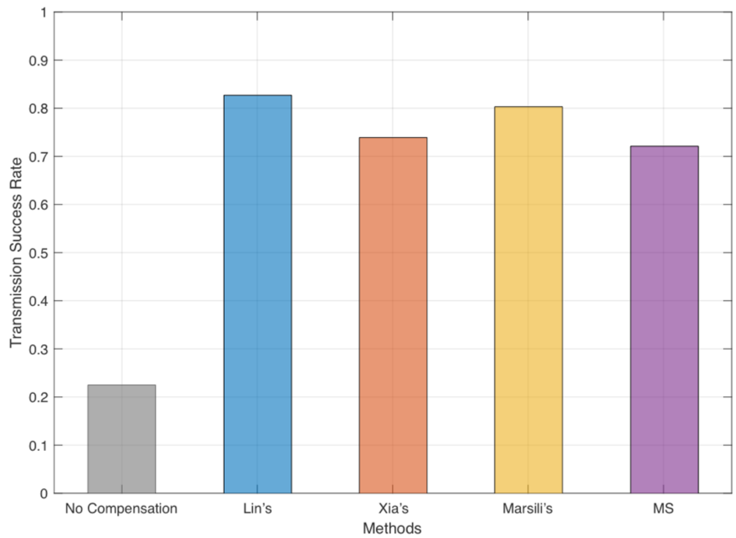

FIGURE 9. Experimental transmission success rates calculated over 1000 trials for the cases where the DC offset is uncompensated and compensated with different methods.

7. CONCLUSIONS

DC offset problem is considered in direct-conversion receivers for WLAN communication systems in this paper. The performance of the DC offset estimation methods have been compared using experimental and simulation data. It has been emphasized that DC offset and frequency offset problems should be considered together for WLAN systems. The results obtained in the paper show that the methods considering CFO values for DC offset estimation can increase the overall system performance. It has been demonstrated that the performance of the DC offset estimation methods depend on the prior information used for the estimation. In this work, data-aided methods have been analyzed for WLAN systems. Blind methods should also be considered for a network in which different wireless protocols are used.

Author Contribution Statements The authors contributed equally to this work.

Declaration of Competing Interests The authors declare that they have no known competing financial interests or personal relationships that could have appeared to influence the work reported in this paper.

Acknowledgement This work was supported by The Scientific and Technological Research Council of Turkey (TUBITAK) under Grant 119E598.

References

[1] Bronckers, S., Roc'h, A., Smolders, B., Wireless Receiver Architectures Towards 5G: Where Are We?, *IEEE Circuits Syst. Mag.*, 17 (3) (2017), 6-16, https://doi.org/10.1109/MCAS.2017.2713306.

[2] Mirabbasi, S., Martin, K., Classical and modern receiver architectures, *IEEE Commun. Mag.*, 38 (11) (2000), 132–139, https://doi.org/10.1109/35.883502.

[3] Razavi, B., Design considerations for direct-conversion receivers, *IEEE Trans. Circuits Syst. II: Analog Digit. Signal Process.*, 44 (6) (1997), 428–435, https://doi.org/10.1109/82.592569.

[4] Abidi, A. A., Direct-conversion radio transceivers for digital communications, *IEEE J. Solid-State Circuits*, 30 (12) (1995), 186–187, https://doi.org/10.1109/4.482187.

[5] Yih, C. -H., Analysis and compensation of DC offset in OFDM systems over frequency-selective Rayleigh fading channels, *IEEE Trans. Veh. Technol.*, 58 (7) (2009), 3436–3446, https://doi.org/10.1109/TVT.2009.2014240.

[6] Xiangning, F., Yutao, S., Yangyang, F., A CMOS DC offset cancellation (DOC) circuit for PGA of low IF wireless receivers, *2010 International Symposium on Signals, Systems and Electronics*, (2010), 1-4, https://doi.org/10.1109/ISSSE.2010.5607078.

[7] Sohn, I. -H., Jeong, E. -R., Lee, Y. H., Data-aided approach to I/Q mismatch and DC offset compensation in communication receivers, *IEEE Commun. Lett.*, 6 (12) (2002), 547-549, https://doi.org/10.1109/LCOMM.2002.806451.

[8] Tseng, H. -Y., Cho, W. -J., Chang, T. -K., Phoong, S. -M., Lin, Y. -P., Compensation of IQ Imbalance and DC Offset for OFDM Transmission over Frequency Selective Channels, *2008 IEEE International Conference on Communications*, (2008), 641–645, https://doi.org/10.1109/ICC.2008.126.

[9] Lin, H., Wang, X. and Yamashita, K., A Low-Complexity Carrier Frequency Offset Estimator Independent of DC Offset, *IEEE Commun. Lett.*, 12 (7) (2008), 520-522, https://doi.org/10.1109/LCOMM.2008.080408.

[10] Xia, Y., Ren, G., A high accuracy DC offset estimation scheme for OFDM based WLAN, *2011 IEEE International Conference on Signal Processing, Communications and Computing (ICSPCC)*, (2011), 1-4, https://doi.org/10.1109/ICSPCC.2011.6061726.

[11] Marsili, S., DC offset estimation in OFDM based WLAN application, *IEEE Global Telecommunications Conference, GLOBECOM '04.*, 6 (2004), 3531–3535, https://doi.org/10.1109/GLOCOM.2004.1379023.

[12] IEEE Std. 802.11, IEEE Standard for Information Technology-Telecommunications and Information Exchange Between Systems Local and Metropolitan Area Networks-Specific Requirements Part 11: Wireless LAN Medium Access Control (MAC) and Physical Layer (PHY) Specifications, 2016.

[13] Lin, H., Sankassa, H. M., Senevirathna, B., Yamashita K., Blind Estimation of Carrier Frequency Offset and DC Offset for OFDM Systems, *IEEE Trans. Commun.*, 56 (5)

(2008), 704-707, https://doi.org/10.1109/TCOMM.2008.060215.

[14] MathWorks, https://www.mathworks.com/help/wlan/, 2022.

[15] Bar-Shalom, Y., Kirubarajan, T., Li, X. -R., Estimation with Applications to Tracking and Navigation, Wiley, New York, 2001.

[16] MathWorks, https://www.mathworks.com/help//supportpkg/plutoradio/ug/transmission and-reception-of-an-image-using-wlan-system-toolbox-and-a-single-pluto-radio.html, 2022.